Available online at www.sciencedirect.com
SCIENCE DIRECT®
Materials Research Bulletin 39 (2004) 1347–1352
Materials Research Bulletin
www.elsevier.com/locate/matresbu

Devitrification of Zr-Ni-Al-Cu-Ti(Nb,Ta) glassy alloys

L.J. Ouyang, D.V. Louzguine[*,1], H.M. Kimura, T. Ohsuna, A. Inoue

Institute for Materials Research, Tohoku University, Katahira 2-1-1, Aoba-Ku, Sendai 980-8577, Japan

Received 20 June 2003; received in revised form 2 March 2004; accepted 3 March 2004

Abstract

The devitrification behavior and phase formation in $Zr_{65-55}Ni_{10}Al_{7.5}Cu_{7.5}Ti_{5-10}(Nb,Ta)_{5-10}$ metallic glass have been studied by X-ray diffraction, transmission electron microscopy and differential scanning calorimetry. It has been found that mutual addition of Ti and Ta/Nb benefits the formation of nanoscale icosahedral phase in the glassy phase on heating and the oxygen content in the alloy makes significant influence on the devitrification behavior of these alloys. At the same time in Nb-bearing alloys and alloys containing 5 at.% Ta icosahedral phase was found to coexist with crystalline one.

Keywords: A. Alloy; A. Quasicrystals; C. Differential scanning calorimetry

1. Introduction

Since the discovery of an icosahedral phase in an Al–Mn alloy, extensive studies on quasicrystals have been carried out in the last years. Quasicrystalline phase has been found in a number of alloys, such as Al-, Mg-, Ga-, Zn-, Ti-, Zr- and Hf-based [1–5].

Quasicrystalline single phase is known to have high hardness [1,6], high corrosion resistance, low coefficient of friction, low adhesion, unique electrical and thermal transport properties, etc. [7–10]. However, it is also known that the quasicrystalline phase is usually extremely brittle [1]. On the other hand, the mixed amorphous alloys containing quasicrystalline particles exhibit good ductility [11,12]. So it is important to search for new alloys with mixed structure containing both amorphous and quasicrystalline phase.

It has been reported that the devitrification behavior of Zr–Al–Ni–Cu glass alloy changes to double-stage from the single-stage one when it contains a certain amount of oxygen (above 1700 mass ppm), and the quasicrystalline phase precipitates as a primary phase [13]. On the other hand, it has also been

* Corresponding author. Tel.: +81-22-2152220; fax: +81-22-2152111.
E-mail address: dml@imr.edu (D.V. Louzguine).
[1] Family name can also be spelt as Luzgin.

0025-5408/$ – see front matter © 2004 Published by Elsevier Ltd.
doi:10.1016/j.materresbull.2004.03.002

reported recently that the quasicrystalline phase precipitates as a primary phase in ZrNiAlCuM (M = Ti, Ag, Au, Pd, Pt, Nb, Ta) [14–19] metallic glasses even at relatively low oxygen content. In the present work, we investigated the devitrification behavior of the $Zr_{65-55}Ni_{10}Al_{7.5}Cu_{7.5}Ti_{5-10}(Nb,Ta)_{5-10}$ glass-forming alloys containing relatively large amount of Ti + Nb or Ti + Ta.

2. Experimental procedure

Ingots of $Zr_{65-55}Ni_{10}Al_{7.5}Cu_{7.5}Ti_{5-10}(Nb,Ta)_{5-10}$ alloys were prepared by arc melting the mixture of pure metals in an argon atmosphere. The oxygen content in the alloys was modified by controlling the vacuum in the chamber during preliminary arc-melting of Zr. Zr actively absorbs O on heating. Amorphous ribbons with a cross-section of about 0.02 mm × 1 mm were prepared by melt spinning technique in an argon atmosphere. The formation of amorphous phase was verified by X-ray diffraction with CuKα radiation. The thermal stability was examined by differential scanning calorimetry at a heating rate of 0.67 K/s. The structure was examined by transmission electron microscopy (TEM) linked with a nanobeam electron diffraction by using a JEM 2010 microscope operating at 200 kV. The sample for TEM observation was prepared by ion-polishing technique. Oxygen content in the studied alloys is examined by infrared absorption method.

3. Results and discussions

The glassy single phase is formed in all of the melt-spun $Zr_{65-55}Ni_{10}Al_{7.5}Cu_{7.5}Ti_{5-10}(Nb,Ta)_{5-10}$ alloys (see e.g., Fig. 1). The melt spun ribbons showed good bend ductility (i.e., showed ability to be bent through 180° without fracture). The oxygen content in the studied alloys is shown in Table 1. The oxygen content in the alloys was modified by controlling the vacuum of the chamber during preliminary arc-melting of Zr.

Fig. 2 shows DSC curves of the $Zr_{65-55}Ni_{10}Al_{7.5}Cu_{7.5}Ti_{5-10}(Nb,Ta)_{5-10}$ alloys. The DSC curves exhibit glass transition at T_g and two exothermic peaks indicating that the devitrification reaction occurs through two stages.

As shown in Fig. 3, the X-ray diffraction patterns of the $Zr_{65-55}Ni_{10}Al_{7.5}Cu_{7.5}Ti_{5-10}(Nb,Ta)_{5-10}$ alloys annealed for 300 s at the temperature of the first exothermic peak consisted of the broad peaks produced by the residual amorphous phase and a few sharp peaks with higher intensities caused by the particles precipitated from the amorphous phase. Due to the small particles size, diffraction peaks

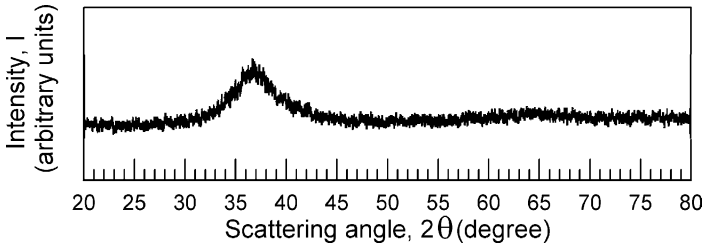

Fig. 1. X-ray diffraction pattern of as-solidified $Zr_{65}Ni_{10}Al_{7.5}Cu_{7.5}Ti_5Nb_5$ ribbon sample.

Table 1
Compositions and oxygen contents in Zr-based glassy alloys used in the present study

Composition (at.%)	O content (mass%)		
	I	II	III
$Zr_{65}Ni_{10}Al_{7.5}Cu_{7.5}Ti_5Nb_5$	0.0575	0.0404	0.0291
$Zr_{55}Ni_{10}Al_{7.5}Cu_{7.5}Ti_{10}Nb_{10}$	0.0557	0.0401	0.0242
$Zr_{65}Ni_{10}Al_{7.5}Cu_{7.5}Ti_5Ta_5$	0.0572	0.0441	0.0206
$Zr_{55}Ni_{10}Al_{7.5}Cu_{7.5}Ti_{10}Ta_{10}$	0.0563	0.0412	0.0245

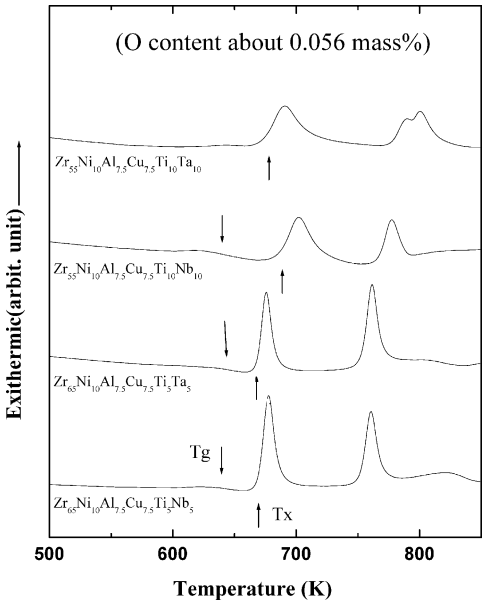

Fig. 2. DSC curves of Zr-based glassy alloys prepared by melt spinning.

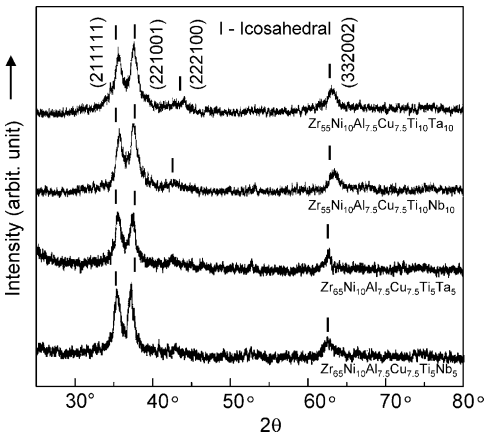

Fig. 3. X-ray diffraction patterns of Zr-based glassy alloys annealed for 300 s at the temperature of the first exothermic peak (O content about 0.056 mass%).

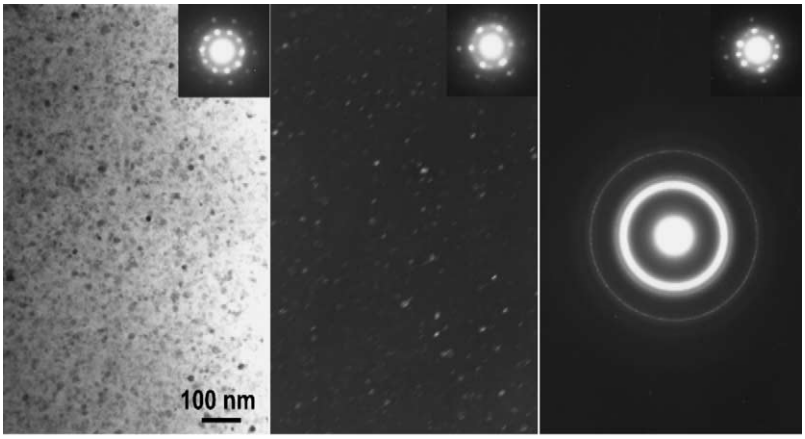

Fig. 4. (a) Bright-field and (b) dark-field TEM images as well as (c) selected-area electron diffraction pattern of $Zr_{55}Ni_{10}Al_{7.5}Cu_{7.5}Ti_{10}Ta_{10}$ glassy alloy annealed for 300 s at 690 K (O content: 0.0563 mass%). The inserts—nanobeam diffraction patterns.

produced by this phase are also quite broad and only four strongest peaks can be identified. Indexing of this icosahedral phase has been done according to Ref. [20].

The structure of the $Zr_{55}Ni_{10}Al_{7.5}Cu_{7.5}Ti_{10}Ta_{10}$ alloy sample annealed for 300 s at 690 K is shown in Fig. 4a and b. The size of the icosahedral particles ranged from 3 to 20 nm. Three sharp rings in the selected-area electron diffraction pattern (Fig. 4c) correspond to the X-ray diffraction peaks. The inserts in Fig. 4 show the nanobeam electron diffraction patterns of the precipitates in $Zr_{55}Ni_{10}Al_{7.5}Cu_{7.5}$-$Ti_{10}Ta_{10}$ alloy. The three kinds of nanobeam electron diffraction patterns reveal five-, three-, and twofold symmetries of the icosahedral quasicrystal. On the other hand, as shown in Fig. 5, relatively

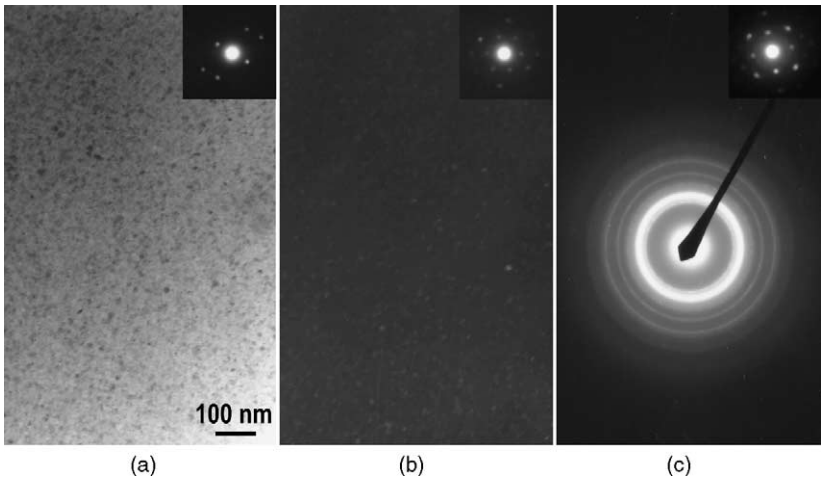

Fig. 5. (a) Bright-field and (b) dark-field TEM images as well as (c) selected-area electron diffraction pattern of $Zr_{65}Ni_{10}Al_{7.5}Cu_{7.5}Ti_5Nb_5$ glassy alloy annealed for 300 s at 678 K (O content 0.0575 mass%). The inserts—nanobeam diffraction patterns.

large precipitates of 10–20 nm in size are identified as nanocrystals in the structure of the $Zr_{65}Ni_{10}Al_{7.5}Cu_{7.5}Ti_5Nb_5$ alloy annealed for 300 s at 678 K while small particles of 3–10 nm in size have an icosahedral symmetry as in the case of $Zr_{55}Ni_{10}Al_{7.5}Cu_{7.5}Ti_{10}Ta_{10}$. The same behavior was observed for $Zr_{55}Ni_{10}Al_{7.5}Cu_{7.5}Ti_{10}Nb_{10}$ and $Zr_{65}Ni_{10}Al_{7.5}Cu_{7.5}Ti_5Ta_5$ alloys. Thus, two kinds of particles precipitated in these alloys, namely, quasicrystalline icosahedral nanoparticles the same as those in the $Zr_{55}Ni_{10}Al_{7.5}Cu_{7.5}Ti_{10}Ta_{10}$ alloy, and larger (10–20 nm in size) cubic nanocrystals. Formation of the icosahedral phase is easily observed by X-ray diffraction due to its large volume fraction. The cubic nanocrystals observed by TEM, however, do not produce peaks in the X-ray diffraction curve (Fig. 3) because of their small volume fraction estimated to be less than 10%. It has also been reported that, in $Zr_{65}Al_{7.5}Ni_{10}Cu_{12.5}Mo_5$ glassy alloy, fcc Zr_2Ni and icosahedral phase can precipitate simultaneously on annealing of the glassy phase [21]. One can suggest that devitrification of the $Zr_{65-55}Ni_{10}Al_{7.5}Cu_{7.5}Ti_{5-10}(Nb,Ta)_{5-10}$ alloys starts from the formation of the icosahedral clustered phase but when it reaches the size of about 10 nm it transforms to a cubic crystalline phase.

We noticed that the oxygen content in $Zr_{55}Ni_{10}Al_{7.5}Cu_{7.5}Ti_{10}Ta_{10}$ alloy is slightly higher than that in the other alloys (see Table 1). In order to study whether oxygen effects the devitrification behavior of these alloys, we prepared two additional groups of $Zr_{65-55}Ni_{10}Al_{7.5}Cu_{7.5}Ti_{5-10}(Nb,Ta)_{5-10}$ alloys with different oxygen content and studied the devitrification behavior of these alloys. In the case of X-ray diffraction and DSC experiments we obtained similar results. The primary precipitating phase examined by TEM in these alloys is reported in Fig. 6. ''Large'' nanocrystals of 10–20 nm in size together with nanoicosahedral particles were observed in $Zr_{55}Ni_{10}Al_{7.5}Cu_{7.5}Ti_{10}Nb_{10}$ alloy and $Zr_{65}Ni_{10}Al_{7.5}Cu_{7.5}Ti_5Nb_5$ alloy at any oxygen content used and in $Zr_{65}Ni_{10}Al_{7.5}Cu_{7.5}Ti_5Ta_5$ alloy, when the oxygen content is low whereas in the $Zr_{55}Ni_{10}Al_{7.5}Cu_{7.5}Ti_{10}Ta_{10}$ alloy the icosahedral phase only is formed at oxygen content as low as 0.0412 mass%. These results indicate that oxygen stabilizes icosahedral phase particles which can have lager size and inhibits the formation of nanocrystals.

We further examined the thermal stability of the precipitated phase by heating the alloys to the temperature of the second exothermic DSC peak. In order to study further structure changes, the $Zr_{65-55}Ni_{10}Al_{7.5}Cu_{7.5}Ti_{5-10}(Nb,Ta)_{5-10}$ alloys were annealed for 300 s at the temperature corresponding to the second exothermic peak (see Fig. 2). The structure of the annealed samples consist of cubic

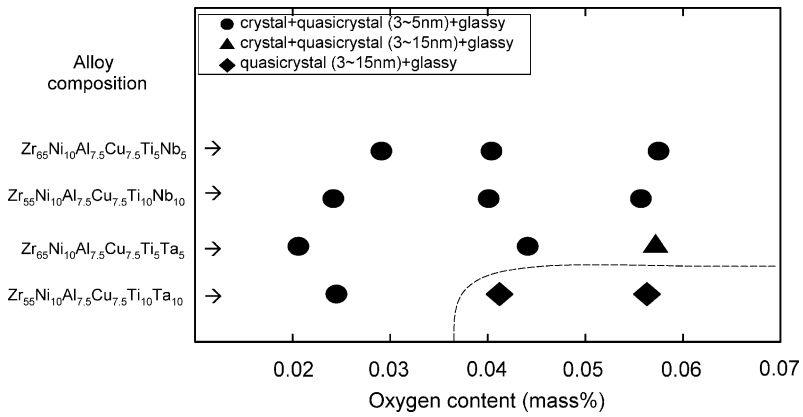

Fig. 6. Phase composition of the studied alloys annealed for 300 s at the temperature of the first exothermic peak as a function of oxygen content.

Zr_2Ni, tetragonal Zr_2Cu and unidentified phases, while no existence of the residual icosahedral phase is observed. Thus, the second exothermic DSC peak in the $Zr_{65-55}Ni_{10}Al_{7.5}Cu_{7.5}Ti_{5-10}(Nb,Ta)_{5-10}$ alloys results from the complicated peritectic-like phase transition from icosahedral + amorphous/icosahedral + nanocrystal + amorphous to cubic Zr_2Ni + tetragonal Zr_2Cu + unidentified phases.

4. Conclusions

The formation of the nanoscale icosahedral and crystalline phases has been observed in the $Zr_{65-55}Ni_{10}Al_{7.5}Cu_{7.5}Ti_{5-10}(Nb,Ta)_{5-10}$ alloys. These alloys showed a double-stage devitrification behavior exhibiting the formation of the icosahedral single phase or icosahedral phase together with nanocrystalline one in the first devitrification stage. The icosahedral single phase embedded in the glassy matrix was formed in the $Zr_{65-55}Ni_{10}Al_{7.5}Cu_{7.5}Ti_{10}Ta_{10}$ alloy at high enough oxygen content. At the same time in Nb-bearing alloys and alloys containing 5 at.% Ta the icosahedral phase was found to coexist with the crystalline one at any oxygen content. With an increase in oxygen content there is a higher tendency for precipitation of the icosahedral single phase within the glassy matrix on annealing at the temperature of the first exothermic DSC peak.

References

[1] S. Takeuchi, Quasicrystals, Sangyotosho, Tokyo, 1992, pp. 81–88.
[2] A.I. Goldman, D.J. Sordelet, P.A. Thiel, J.M. Dubois (Eds.), New Horizons in Quasicrystals, World Scientific, Singapore, 1997, pp. 1–85.
[3] A. Inoue, T. Zhang, J. Saida, M. Matsushita, M.W. Chen, T. Sakurai, Mater. Trans. JIM 40 (1999) 1137.
[4] D.V. Louzguine, M.S. Ko, A. Inoue, Appl. Phys. Lett. 76 (2000) 3424.
[5] J.Z. Jiang, K. Saksl, J. Saida, A. Inoue, H. Franz, K. Messel, C. Lathe, Appl. Phys. Lett. 80 (2002) 781.
[6] S. Takeuchi, Iron and Steel, 1992, p. 1517.
[7] F.S. Pierce, S.J. Poon, Q. Guo, Science 261 (1993) 737.
[8] C. Janot, Phys. Rev. B 53 (1996) 181.
[9] T. Eisenhammer, Thin Solid Films 270 (1995) 1.
[10] M. Feuerbacher, C. Metzmacher, M. Wollgarten, K. Urban, B. Baufeld, M. Bartsch, U. Messerschmidt, Mater. Sci. Eng. A226 (1997) 943.
[11] K. Kita, K. Saitoh, A. Inoue, T. Masumoto, Mater. Sci. Eng. A226 (1997) 1004.
[12] A. Inoue, H.M. Kimura, K. Kita, Proceedings of the Sixth International Conference on Quasicrystals, Tokyo, 1997, p. 723.
[13] U. Koster, J. Meinhardt, S. Roos, H. Liebertz, Appl. Phys. Lett. 69 (1996) 179.
[14] M.W. Chen, T. Zhang, A. Inoue, A. Sakai, T. Sakurai, Appl. Phys. Lett. 75 (1999) 1697.
[15] A. Inoue, T. Zhang, M.W. Chen, T. Sakurai, Mater. Trans., JIM 40 (1999) 1382.
[16] A. Inoue, T. Zhang, M. Matsushita, M.W. Chen, T. Sakurai, Mater. Trans., JIM 40 (1999) 1137.
[17] L.Q. Xing, J. Ecket, L. Schultz, Appl. Phys. Lett. 73 (1998) 2110.
[18] C. Fan, A. Inoue, Scripta Materialia 45 (2001) 115.
[19] J. Saida, A. Inoue, J. Phys. Condens. Matter 13 (2001) L73.
[20] V. Elser, Phys. Rev. B 32 (1985) 4892.
[21] J. Saida, A. Inoue, Jpn. J. Appl. Phys. 40 (2001) L769.